

2-DIMENSIONAL NUMERICAL CALCULATION OF FLOW AND MIXING USING THE CIP METHOD

By

Ryosuke AKAHORI

Division of Environment and Resource Engineering, Faculty of Engineering,
Hokkaido University, Sapporo, Japan

Yasuyuki SHIMIZU

Associate Professor, Division of Environment and Resource Engineering, Faculty of Engineering,
Hokkaido University, Sapporo, Japan

and

Suguru NAKAYAMA

Division of Environment and Resource Engineering, Faculty of Engineering,
Hokkaido University, Sapporo, Japan

SYNOPSIS

Numerical models are useful to predict the characteristics of environmental systems at the interface between waters of different densities. In the last few years, some models have been proposed to calculate factors including flow in stratified and closed water systems and saltwedges. They provided favorable results. Models that analyze the flow of waters of different densities are needed to accurately calculate density distribution. However, models that take an ordinary finite differential method suffer from a major difficulty in calculating the advection term because numerical diffusion. In this paper, a simple two-dimensional numerical model is constructed. The model uses the CIP method in the calculation of advection term, in order to calculate density flows more accurately without using complicated models. The model applicability was verified by the comparison between the calculation and the experimental results under the same condition.

INTRODUCTION

Characteristic phenomena occur at the interface between water layers of different densities. These include "aoshio" in a stratified water system and salt wedge encroachment at a river mouth. A numerical model is useful to understand the characteristics of environmental systems of such phenomena and to predict the causes. In the last few years, many numerical models of density flow have been proposed. Examples are the study of hydraulic characteristics in semi-enclosed stratified basins by $k - \epsilon$ model (Michioku (1)), the simulation of behavior of the density interface between salt and fresh waters in Lake Abashiri by the multilayer model (Ikenaga (2)), and the numerical analysis of a density front in a densimetric exchange flow (Hosoda (3)). These models realized favorable results.

A numerical simulation would aim a precise solution at the density interface between fluids. However, a numerical model that employs an ordinary upwind scheme suffers from numerical diffusion when it calculates advection term, and this numerical diffusion overstates density diffusion, especially at the interface. Therefore, this study proposes a new numerical model to calculate density flow more accurately by using the CIP method (Yabe (4)), which has recently gained attention in the field of computational fluid dynamics. The method was used to simulate the density front advance and the internal seiche by the direct calculation with a simple model of 2-dimensional incompressible flow, which is based on Navier-Stokes equations. Since turbulent flow is originally

3-dimensional, a turbulence models or the Direct Numerical Simulation is needed for flow simulation. However, in this study, a 2-dimensional model is used for simplification of analysis, because present flow systems were regarded as roughly 2-dimensional and because we aimed to provide a model whose calculations are possible by PC.

In this method, values in the next computational step are interpolated from profiles of physical quantities in the computational domain. The profiles are approximated by a cubic equation that is defined from the latest variables on the grids. The CIP method (4) is able to calculate density distribution at the interface more precisely than the upwind scheme. Recently, many applications of the CIP were provided in the several fields of engineering (Yabe (5), (6)). The model in this study is very simple; however it is expected to be very precise, for the reasons above mentioned.

The results of the calculation and the experiment under the same condition were compared to verify the model. The numerical results successfully reproduced the phenomena.

BASIC EQUATIONS

The basic equations of a vertical 2-dimensional, numerical model of incompressible density flow are shown below. Eq.1 is the continuity equation, Eq.2 and Eq.3 are the Navier-Stokes equations, and Eq.4 is a density equation. Eq.4 is obtained from Eq.1 and from a continuity equation of salt concentration c that includes advection and diffusion terms. To obtain Eq.4, a relationship ($c = (\rho - \rho_w)/\rho_w$, ρ is density and ρ_w is fresh water density) must be substituted into in the conservation equation of salinity c .

$$\frac{\partial u}{\partial x} + \frac{\partial v}{\partial y} = 0 \quad (1)$$

$$\frac{\partial u}{\partial t} + u \frac{\partial u}{\partial x} + v \frac{\partial u}{\partial y} = -\frac{\partial P}{\partial x} + \nu \left(\frac{\partial^2 u}{\partial x^2} + \frac{\partial^2 u}{\partial y^2} \right) \quad (2)$$

$$\frac{\partial v}{\partial t} + u \frac{\partial v}{\partial x} + v \frac{\partial v}{\partial y} = -\frac{\partial P}{\partial y} + \nu \left(\frac{\partial^2 v}{\partial x^2} + \frac{\partial^2 v}{\partial y^2} \right) - g \quad (3)$$

$$\frac{\partial \rho}{\partial t} + u \frac{\partial \rho}{\partial x} + v \frac{\partial \rho}{\partial y} = D_x \frac{\partial^2 \rho}{\partial x^2} + D_y \frac{\partial^2 \rho}{\partial y^2} \quad (4)$$

Here, (x, y) are orthogonal axes, $P = p/\rho$ (p is pressure), g is gravitational acceleration, u and v are velocity components on x and y axes, t is time, ν is a coefficient of viscosity, D_x, D_y are coefficients of diffusion on x and y axis.

In this paper, the computational domain is defined in a body-fitted coordinate system (ξ, η) instead of in the Cartesian coordinate (x, y) to enable calculation of complicated lakes of arbitrary shape. The boundaries of the body-fitted coordinate are the water surface line and the bottom line of a lake. On the coordinate, ξ axis is set along the water and along the bottom line and η axis is taken positive upward. These axes are defined as follows: $x = x(\xi, \eta, \tau)$, $y = y(\xi, \eta, \tau)$, $t = \tau$.

Eq.5 or Eq.6 describes the relationship between these two coordinate systems.

$$\begin{pmatrix} \frac{\partial}{\partial t} \\ \frac{\partial}{\partial x} \\ \frac{\partial}{\partial y} \end{pmatrix} = \begin{pmatrix} 1 & \xi_t & \eta_t \\ 0 & \xi_x & \eta_x \\ 0 & \xi_y & \eta_y \end{pmatrix} \begin{pmatrix} \frac{\partial}{\partial \tau} \\ \frac{\partial}{\partial \xi} \\ \frac{\partial}{\partial \eta} \end{pmatrix} \quad (5)$$

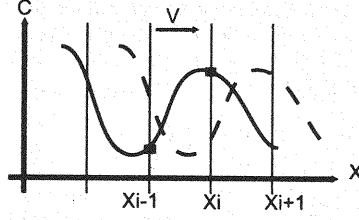
$$\begin{pmatrix} \frac{\partial}{\partial \tau} \\ \frac{\partial}{\partial \xi} \\ \frac{\partial}{\partial \eta} \end{pmatrix} = \begin{pmatrix} 1 & x_\tau & y_\tau \\ 0 & x_\xi & y_\xi \\ 0 & x_\eta & y_\eta \end{pmatrix} \begin{pmatrix} \frac{\partial}{\partial t} \\ \frac{\partial}{\partial x} \\ \frac{\partial}{\partial y} \end{pmatrix} \quad (6)$$

By these relationships, Eqs.1~4 are transformed into Eqs.8, 9, 10, and 11. New coordinates are now introduced as:

$$\tau = t, \quad \xi = x, \quad \eta = (y - z)/h \quad (7)$$

in which, z is height from the bottom and $h = H_{wt} - z$, where H_{wt} is water level and h is water depth.

$$\frac{\partial}{\partial \xi}(hu) + \frac{\partial}{\partial \eta}(v_1) = 0 \quad (8)$$

Fig.1 Transportation of C

$$\frac{\partial u}{\partial \tau} + u \frac{\partial u}{\partial \xi} + v_2 \frac{1}{h} \frac{\partial u}{\partial \eta} = - \left(\frac{\partial P}{\partial \xi} - \frac{\Omega}{h} \frac{\partial P}{\partial \eta} \right) + \nu \Delta u \quad (9)$$

$$\frac{\partial v}{\partial \tau} + u \frac{\partial v}{\partial \xi} + v_2 \frac{1}{h} \frac{\partial v}{\partial \eta} = - \frac{1}{h} \frac{\partial P}{\partial \eta} + \nu \Delta v - g \quad (10)$$

$$\frac{\partial \rho}{\partial t} + u \frac{\partial \rho}{\partial \xi} + v_2 \frac{1}{h} \frac{\partial \rho}{\partial \eta} = D_x \left(\frac{\partial^2 \rho}{\partial \xi^2} - 2\Omega \frac{1}{h} \frac{\partial^2 \rho}{\partial \xi \partial \eta} \right) + D_y \frac{1}{h^2} \frac{\partial^2 \rho}{\partial \eta^2} \quad (11)$$

where,

$$v_1 = v - u\Omega, \quad v_2 = v_1 - \eta \frac{\partial h}{\partial \tau}, \quad \Omega = \eta \frac{\partial h}{\partial \xi} + \frac{\partial z}{\partial \xi} \quad (12)$$

$$\Delta = \frac{\partial^2}{\partial \xi^2} + \frac{1}{h^2} \frac{\partial^2}{\partial \eta^2} - 2\frac{\Omega}{h} \frac{\partial^2}{\partial \xi \partial \eta} - \frac{1}{h} \frac{\partial \Omega}{\partial \xi} \frac{\partial}{\partial \eta} \quad (13)$$

THE CIP METHOD (4)

The CIP method(4) is a main part of this model. Here, for briefly showing the basic idea of the CIP method, 1-dimensional wave equation, Eq.14 is considered instead of a 2-dimensional system.

$$\frac{\partial C}{\partial t} + V \frac{\partial C}{\partial x} = 0 \quad (14)$$

This equation suggests that a value C is convected by a velocity V , while keeping its profile in the x axis (Fig.1).

However, since the value C is known only at grid points, a profile between grid points must be assumed in order to obtain a value in the next time step.

In the CIP method (4), every two successive grid points located on the curved line are approximated by a cubic equation(15), in which, a_i , b_i , C_i' are still unknown.

$$F_i(x) = a_i(x - x_i)^3 + b_i(x - x_i)^2 + C_i'(x - x_i) + C_i \quad (15)$$

First, a_i and b_i are obtained from Eqs.16 and 17 as in Eqs.18 and 19. Eq.16 means that a value of C is continuous on the grid points and Eq.17 means that first derivative of C is also continuous on the grid points as well.

$$F_i(x_{i-1}) = F_{i-1}(x_{i-1}) \quad (16)$$

$$dF_i(x_{i-1})/dx = dF_{i-1}(x_{i-1})/dx \quad (17)$$

$$a_i = \frac{C_i' + C_{i+1}'}{\delta x^2} - 2 \frac{C_{i+1} - C_i}{\delta x^3} \quad (18)$$

$$b_i = 3 \frac{C_{i-1} - C_i}{\delta x^2} + \frac{2C_i' + C_{i-1}'}{\delta x} \quad (19)$$

From these equations, it is recognized that a_i and b_i can related to by C and C' .

However, the three unknowns (a_i , b_i , C_i) cannot be determined from these two equations, yet. Therefore, it is assumed that C'_i , the derivative of C_i , is conserved while it is convected with a velocity V , in other words, C'_i satisfies a relationship $C'_i(x, t) = C'_i(x - \delta t, t - \delta t)$. This is deduced concluded from Eq.20. The same thing can be recognized also in the relationship of C between the equation $C(x, t) = C(x - \delta t, t - \delta t)$ and Eq.14.

$$\frac{\partial C'}{\partial t} + V \cdot \frac{\partial C'}{\partial x} = 0 \quad (20)$$

Now, C and C' are known, then a_i and b_i are obtained by Eqs.18 and 19.

The values in the next time step, C_i^{new} and $C_i'^{new}$, can be obtained from Eq.21 and Eq.22 by using a_i and b_i ,

$$C_i^{new} = F_i(x_i - V\delta t) = [(a_i\xi + b_i)\xi + C_i']\xi + C_i \quad (21)$$

$$C_i'^{new} = \frac{F_i(x_i - V\delta t)}{dx} = (3a_i\xi + 2b_i)\xi + C_i' \quad (22)$$

in which, $\xi = (-V\delta t)$.

In the actual calculation, the same method is applied to the 2-dimensional system, and the advection term in the basic equations is calculated by using so-called "separation method".

CALCULATION PROCEDURE

Eq.9, Eq.10, and Eq.11 are calculated by the separation method, so that the CIP method (4) can be used. The procedure is as follows.

At first, Eq.9, 10, and 11 are transformed into finite differential forms and divided into the advection term and others. Except for advection, Eqs.9 and 10 are also divided into two parts: viscosity term and others including pressure gradient. These terms are calculated step by step. In this procedure, the part including pressure term can be solved by a Poisson equation with SOR method so as Eq.8 to be satisfied. In the separation method, the pressure term is neither advective nor diffusive. So the Poisson equation has a very simple structure.

Next, the advection term is calculated by the CIP method (4), and in the next time step values such as velocity and density are obtained.

At the boundaries of bottom and walls, non-slip condition is applied, and the water surface is considered to be free from shear. Water surface variation is regarded as very small and it is approximated to be rigid in this paper.

OVERVIEW OF THE EXPERIMENT

Fig.(2) outlines the experimental setup. Length of the flume is 1.0(m), width 0.4(m), height 0.3(m), and water depth is 0.155(m). At first, the flume is divided into left and right blocks by a plastic partition at the center of the flume, where the left side is filled with fresh water and the right side with salt water, respectively. The salt water is dyed blue. Density of water on the left side is 1000.0(kg/m³) and on the right side is 1033.0(kg/m³). At time $t=0.0$ (sec), the partition is quickly removed and the water from both sides starts to form layers. This motion is recorded by digital video camera, and the image data is stored in a desktop computer. These images are compared with the calculation result.

Actual saltwedge is usually found, constructed in an open water system. However, our model addresses a closed water system, and the main purpose of the experiment is verification of the numerical model. Therefore, both of the numerical and experimental models are set in a closed water system.

RESULTS OF THE EXPERIMENT

Fig.3 shows the results of the experiment obtained from the motion picture.

At $t=0.0$ (sec), when the central partition is removed, the salt water plunges into the fresh water, and the density front starts to move. Then two swells are observed at the front and at the middle of the interface (arrows in Fig.3). These swells are considered to be vortices generated by the interfacial shear stress. Density diffusion is observed right behind these vortexes. The front reaches the left end at about $t=6.0$ (sec), and the

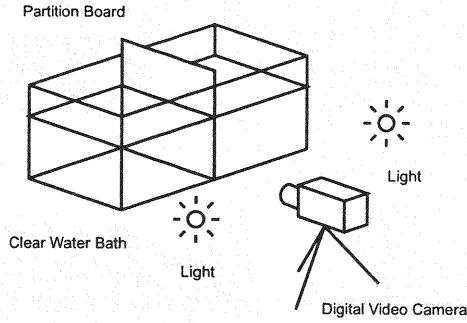


Fig.2 Overview of Experimental Setup

density water rises up to its highest point at about $t=12.0(\text{sec})$. Then, the internal seiche is generated. The seiche's period is about $24(\text{sec})$.

INITIAL CONDITION OF THE CALCULATION

Fig.4 shows the initial condition of the calculation. The numerical results obtained under the following conditions are compared with the experiment.

Height of the computational domain is $0.155(\text{m})$, and length is $1.0(\text{m})$. The flume is divided into two blocks at first. Water density of left side ρ_1 is $1000.0(\text{kg}/\text{m}^3)$, that of right side ρ_2 is $1033.0(\text{kg}/\text{m}^3)$. The center partition is removed when the calculation starts at $t=0.0(\text{sec})$.

Beside, the fluid viscosity is $\nu = 0.000001(\text{m}^2/\text{s})$ for water temperature of 20 degrees Celsius, the diffusion coefficients are $D_x = D_y = 0.000001(\text{m}^2/\text{s})$, and numbers of grid points are 30 in the vertical direction, 100 in the horizontal direction, respectively.

CALCULATION RESULTS

Fig.5 shows the results of calculation. These are compared only graphically with the experiment, because it is very difficult to collect precise data of velocity or density in the experiment. However, this comparison is enough to show the model's performance. In Fig.5, the darker pattern indicates higher density, and black dots are tracers.

At $t=0.0(\text{sec})$, the density front is shaped immediately and starts to migrate to the left side. While the front advances, vortices gradually grow along the deformable density interface, and water density difference diffuse mainly behind the vortices. Calculation of this process agreed well with results of the experiment. In addition, the vortices caused by the shear stress are observed very clearly in calculation (arrows in Fig.5), and their locations are close to those in the experiment. Then, the front reaches the left end of the channel, and after the dense water rising to its highest point at about $t=12.0(\text{sec})$, internal seiche is generated. The period of seiching is about $23(\text{sec})$. The behavior of seiche and its period time are also very similar to those of the experiment.

In Figs.6 and 7, our calculations are compared with past similar experiments and calculations from previous other research. Our model's availability is confirmed through comparison. To plot more data (like mixed layer thickness at the front, lower layer thickness, and Reynolds number), other three calculations are done with our model, where the initial water depth are decreased by $2.0(\text{cm})$ gradually in each case. All other initial conditions are the same as for the first calculation mentioned above. The objects of comparison are the calculations results of numerical analysis of a density front in a densimetric exchange flow by Hosoda (3), which is mentioned in introduction, and results of experiments by Simpson, Britter (7) and by Okubo (8). These experiments are quoted in Hosoda (3). This comparison is not so strict, because conditions of the calculations and experiments are different from our calculations. However, the comparison is supposed to show the tendency of the density front profile.

Fig.6 shows the relationship between the Reynolds number and the mixed layer thickness, in which, H is the water depth, h_3 is a mixed layer thickness, h_4 is lower layer, Re is defined as: $Re = u_2 R / \nu$ (R is a hydraulic

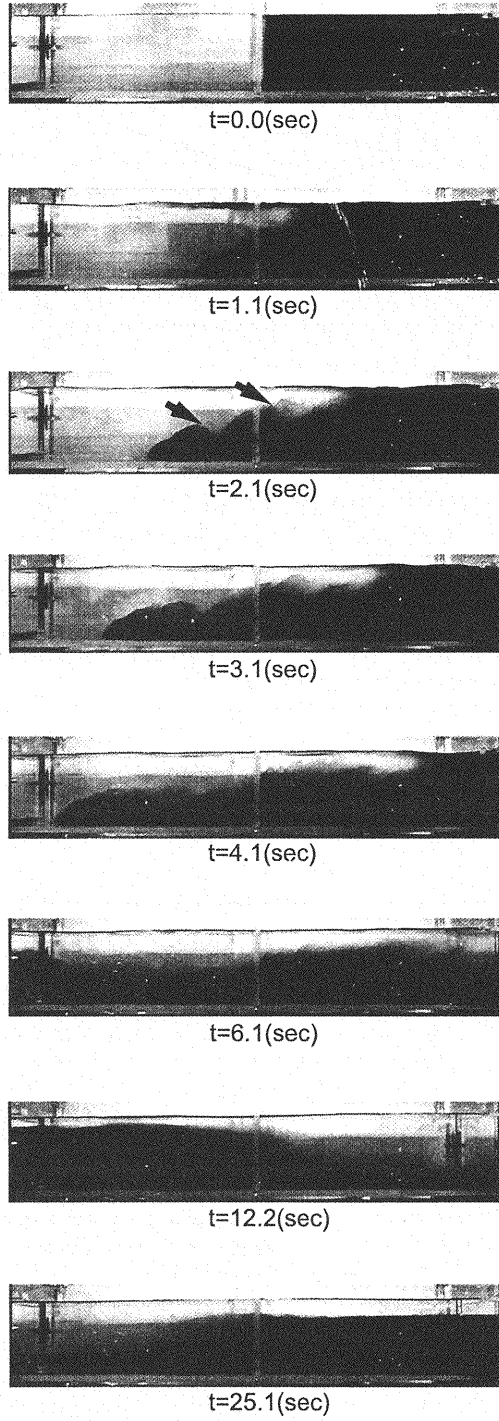


Fig.3 Experimental Results

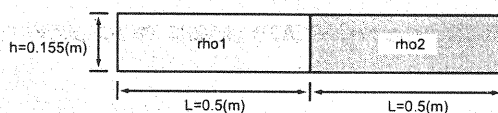


Fig.4 Initial Condition

radius of the lower layer as defined in Okubo's experiment and identified to be $H/4$ in calculations), and u_2 is the density front velocity. In this figure, we can compare the mixed layer thickness of our calculations providing better agreement with the experiment than those of previous calculations. In the experiments (7)(8), optical and chemical techniques were used, and only the mixed layer was measured

Fig.7 shows the relationship between the mixed layer thickness and the lower layer thickness. In this figure, it is concluded that our calculation results agree with experimental results such as mixing events across the density interface.

CONCLUSIONS

In this paper, a simple and precise 2-dimensional numerical model employing the CIP method (4) was constructed to calculate density flows, and this model applicability was tested by comparison between calculation results and experimental results under similar conditions or past calculations and experiments by other researchers.

Regarding comparison between calculation results and experimental results under similar conditions, the method was brief. However, this numerical model agreed well with the experiment. In particular, the advance of the vortices behind the density front was observed more clearly in the model calculations than in the experiment. Besides, the behavior of internal seiche, which plays a very important role in hydraulics at the stratified fluids, could be reproduced on the laboratory scale.

Otherwise, through comparison between our model's result and those from previous experiments and calculations by others, our model using the CIP method (4) could provide more accurate result. The CIP was recognized to be a good tool for decreasing the mixed layer thickness, which is caused by too much numerical diffusion. The successful results were thanks to the CIP method (4), which can reproduce interfacial events with high resolution.

This study showed that a simple numerical model, which employs the CIP method (4), is applicable to complicated phenomena such as of density flows. This model is expected to be a powerful tool to simulate behavior of interface of different density waters.

REFERENCES

1. Michioku, K., G. Tsujimoto, and H. Miyamoto : Water exchange characteristics of wind-driven density current system in semi-enclosed stratified basins, Annual Journal of Hydraulic Engineering, Vol.39, pp.805-810, 1995. (in Japanese)
2. Ikenaga, H., T. Yamada, K. Uchijima, K. Mukouyama, M. Hirano, and Y. Ide : Study on generation of wind-driven current and behavior of the density interface between salt and fresh waters in Lake Abashiri, Annual Journal of Hydraulic Engineering, Vol.41, pp.481-488, 1997. (in Japanese)
3. Hosoda, T., K. Nishizawa, A. Fukusumi, K. Okubo, and Y. Muramoto : Numerical studies on internal waves induced in a densimetric exchange flow, Annual Journal of Hydraulic Engineering, Vol.40, pp.525-530, 1996. (in Japanese)
4. Yabe, T. and T. Aoki : A universal solver for hyperbolic equations by cubic-polynomial interpolation I. One-dimensional solver, Comp. Phys. Comm., Vol.66, pp.219-232, 1991.
5. Yabe, T. and F. Xiao : CIP method: a unified solver of solid, liquid and gas (1), Japan Society of CFD, vol.7 No.2, pp.70-81, 1999. (in Japanese)
6. Yabe, T. and F. Xiao : CIP method: a unified solver of solid, liquid and gas (2), Japan Society of CFD, vol.7 No.3, pp.103-114, 1999. (in Japanese)
7. Simpson, J. E. and R. E. Britter : The dynamics of the head of a gravity current advancing over a horizontal surface, J. Fluid Mech., Vol.94, pp.477-495, 1979.

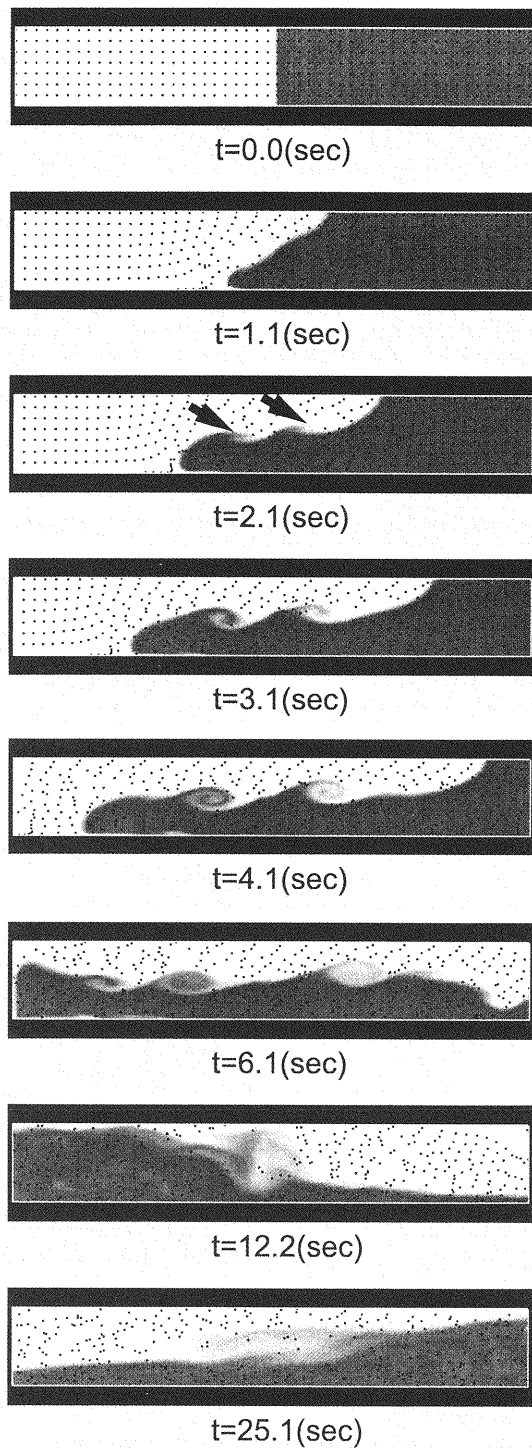


Fig.5 Calculation Results

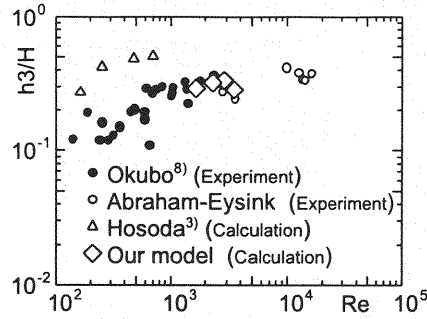


Fig.6 Relationship between Reynolds Number and Mixed Layer Thickness

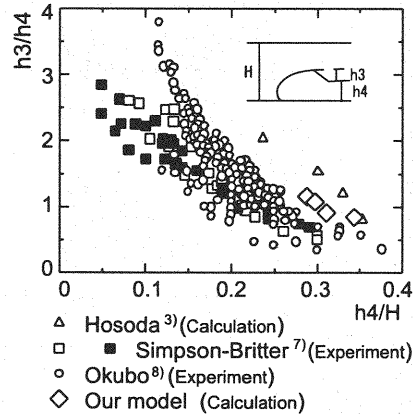


Fig.7 Relationship between Mixed Layer Thickness and Lower Layer Thickness

8. Okubo, K. : A study of generation and hydraulic mechanics of wind driven current and density flow in lakes, Dissertation of Kyoto Univ., 1988. (in Japanese)

APPENDIX - NOTATION

The following symbols are used in this paper:

c	=	concentration;
ρ	=	density;
ρ_w	=	fresh water density;
u	=	velocity components on x direction;
v	=	velocity components on y direction;
x, y	=	orthogonal axes;
t	=	time;
P	=	pressure / density;
ν	=	coefficient of viscosity;
g	=	gravitational acceleration;
D_x	=	coefficients of diffusion on x direction;
D_y	=	coefficients of diffusion on y direction;
ξ, η	=	axes on body-fitted coordinates;

τ	=	time;
ξ_t	=	$\partial \xi / \partial t$;
η_t	=	$\partial \eta / \partial t$;
ξ_x	=	$\partial \xi / \partial x$;
η_x	=	$\partial \eta / \partial x$;
ξ_y	=	$\partial \xi / \partial y$;
η_y	=	$\partial \eta / \partial y$;
x_τ	=	$\partial x / \partial \tau$;
y_τ	=	$\partial y / \partial \tau$;
x_ξ	=	$\partial x / \partial \xi$;
y_ξ	=	$\partial y / \partial \xi$;
x_η	=	$\partial x / \partial \eta$;
y_η	=	$\partial y / \partial \eta$;
z	=	bottom level;
h	=	water depth;
H_{wl}	=	water level;
v_1	=	defined as Eq.(12);
v_2	=	defined as Eq.(12);
Ω	=	defined as Eq.(12);
V	=	velocity on 1-dimensional wave equation;
C	=	a value transported by V ;
F_i	=	cubic function providing profile of C between grid points $i - 1$ and i ;
a_i	=	unknown value in Eq.(15);
b_i	=	unknown value in Eq.(15);
C_i	=	C on grid points;
C'_i	=	derivative of C_i ;
x_i	=	position on grid points
ρ_1	=	water density in left side of the flume;
ρ_2	=	water density in right side of the flume;
H	=	total water depth;
h_3	=	mixed layer thickness;
h_4	=	lower layer thickness;
u_2	=	front velocity; and
R	=	hydraulic radius.

(Received November 15, 1999 ; revised February 22, 2000)